Electrochemistry of Chlorinated Ferrocenes: Stability of Chlorinated Ferrocenium Ions†

Kylie N. Brown, Peter T. Gulyas, Peter A. Lay,* Neale S. McAlpine, Anthony F. Masters and Leonidas Phillips
Department of Inorganic Chemistry, University of Sydney, 2006 NSW, Australia

---

The cyclic voltammetries of 1,2,3,4,5-pentachloro- and decachloro-ferrocene have been studied in acetonitrile. The complexes undergo an irreversible two-electron oxidation consistent with an electrochemical–chemical–electrochemical mechanism at scan rates up to 10 V s^{-1}. However, at the faster scan rates (up to 160 V s^{-1}) available to electrodes of small radius and microelectrodes, chemically reversible one-electron oxidations to the chlorinated ferrocenium ions, [$C_{10}H_{10-x}Cl_xFe$]$^+$ are obtained under ambient conditions. The reversible [$C_{10}H_{10-x}Cl_xFe$]$^{+/0}$ couples when x = 10, 5, 2 and 1 are observed at +1.246, +0.774, +0.315 and +0.168 V *vs.* ferrocenium–ferrocene, respectively. A plot of E_f *vs.* $\Sigma\sigma_p$ (σ_p = Hammett *para* coefficient for the chloro substituent) shows that the neutral molecules are stabilised with respect to the corresponding ferrocenium cations by 0.16–0.12 V per Cl. The rate constants of decomposition of the [Fe(η-C_5Cl_5)$_2$] and [Fe(η-C_5H_5)(η-C_5Cl_5)]$^+$ cations were calculated by both digital simulation and the method of Nicholson and Shain to be 40 ± 20 and 200 ± 50 s^{-1}, respectively, at room temperature (*ca.* 20 °C). The complexes [Fe(η-C_5H_4Cl)$_2$] and [Fe(η-C_5H_5)(η-C_5H_4Cl)] exhibit reversible oxidations at all scan rates down to 0.100 V s^{-1} under the same conditions. Both [Fe(η-C_5Cl_5)$_2$] and [Fe(η-C_5H_5)(η-C_5Cl_5)] undergo a series of irreversible two-electron reductions at potentials negative of −1.8 V, which lead to reductive dechlorination consistent with an electrochemical–chemical–electrochemical–chemical reaction.

Ferrocene and its analogues have been the subject of extensive electrochemical studies since the early 1950s.[1–4] The mechanism of interaction between substituents and the metallocene iron centre has been studied using correlations between the formal Fe^{III}–Fe^{II} redox potentials (E_f) of ferrocene and substituent coefficients such as the Hammett *para* (σ_p) and *meta* (σ_m) coefficients.[5] These studies revealed strongest correlations between E_f and σ_p.[4d,5c,6]

Kuwana *et al.*[5b] showed that, in acetonitrile, electron-donating substituents (*e.g.* CH_3) resulted in a negative shift in E_f relative to the ferrocenium–ferrocene couple (IUPAC[7] internal reference). The opposite effect occurs for electron-withdrawing groups (*e.g.* Cl). Fewer studies exist on the reduction chemistry of ferrocene, however a quasi-reversible reduction is observed at −30 °C in dimethylformamide (dmf) to yield the ferrocene anion, which is stable on the minutes time-scale.[3,4b,8] Electrochemical reductions of various substituted ferrocenes have also been reported.[9]

Although an extensive literature exists on ferrocene electrochemistry, few publications focus on highly substituted ferrocenes with strong electron-withdrawing substituents. Although decachloroferrocene [Fe(η-C_5Cl_5)$_2$] and 1,2,3,4,5-pentachloroferrocene [Fe(η-C_5H_5)(η-C_5Cl_5)] have been the subject of a range of spectroscopic and physical studies,[10] the electrochemical oxidation of the former has been mentioned only in a communication dealing with the correlation between gas-phase ionisation potentials and E_f.[6b] No extensive electrochemical studies have been reported previously on these complexes, but because of the strong electron-withdrawing properties of the chloro substituents the chlorinated ferrocenium analogues are expected to be strong oxidants. The species were also of interest for possible stabilisation of the anionic members of the redox series. Here, the cyclic voltammetries, decomposition kinetics of the cations, and protonation chemistries of [Fe(η-C_5Cl_5)$_2$] and [Fe(η-C_5H_5)(η-C_5Cl_5)] are reported. The effects of chlorination upon the reductive properties of the chloro-substituted ferrocenes are also examined.

Results and Discussion

Oxidation Chemistry and Formal Redox Potentials.—Fig. 1 shows the cyclic voltammograms of the oxidations of [Fe(η-C_5Cl_5)$_2$], [Fe(η-C_5H_5)(η-C_5Cl_5)], [Fe(η-C_5H_4Cl)$_2$] and [Fe(η-C_5H_5)(η-C_5H_4Cl)] in acetonitrile–0.1 mol dm^{-3} tetrabutylammonium tetrafluoroborate using a glassy carbon electrode at a scan rate of 0.100 V s^{-1}. The oxidations of [Fe(η-C_5H_4Cl)$_2$] and [Fe(η-C_5H_5)(η-C_5H_4Cl)] are electrochemically and chemically reversible with cathodic to anodic peak current ratios (i_{pc}/i_{pa}) close to unity. Comparison of ΔE_p and peak currents for both couples to those of ferrocenium–ferrocene under similar conditions is consistent with reversible one-electron oxidation for both couples. The E_f values were found to be 0.315 (ΔE_p = 60) and 0.168 V (55 mV) *vs.* ferrocenium–ferrocene, for [Fe(η-C_5H_4Cl)$_2$] and [Fe(η-C_5H_5)(η-C_5H_4Cl)], respectively. The oxidations of [Fe(η-C_5Cl_5)$_2$] and [Fe(η-C_5H_5)(η-C_5Cl_5)] under identical conditions were irreversible. Cyclic voltammograms obtained at higher scan rates using both conventional electrodes and microelectrodes (see below) showed irreversibility of both couples at scan rates up to 10 V s^{-1}. This indicates rapid decomposition of the [Fe(η-C_5Cl_5)$_2$]$^+$ and [Fe(η-C_5H_5)(η-C_5Cl_5)]$^+$ cations under these conditions. Formal redox potentials of the [Fe(η-C_5Cl_5)$_2$]$^{+/0}$ and [Fe(η-C_5H_5)(η-C_5Cl_5)]$^{+/0}$ couples were obtained at scan rates between 80 and 160 V s^{-1}. Voltammetric data obtained for all chlorinated ferrocenes (*vs.* ferrocenium–ferrocene) along with relevant experimental details are given in Table 1.

Increased cyclopentadienyl ring substitution by the chloro

---

† *Supplementary data available* (No. SUP 56925, 7 pp.): primary kinetic data, simulated cyclic voltammograms and peak current plots. See Instructions for Authors, *J. Chem. Soc., Dalton Trans.*, 1993, Issue 1, pp. xxiii–xxviii.

Non-SI unit employed: eV ≈ 1.60 × 10^{-19} J.

Table 1 Voltammetric data for the oxidation and reduction of $C_{10}H_{10-x}Cl_xFe$ (x = 1, 2, 5 or 10) in MeCN–0.1 mol dm^{-3} NBu_4BF_4[a]

		ΔE_p			
x	E_f[b]	c	d	E_{pa}[e]	E_{pc}[f,g]
10	1.246[h]	0.098	0.083	*ca.* 1.53[i]	−1.809, −1.898, −1.992, −2.097, −2.235, −2.358, −2.533, −2.683
5	0.774[j]	0.100	0.100	1.148[k]	−2.332, −2.524, −2.729
2	0.315[g]	0.060	0.050		
1	0.168[g] (0.165)[l]	0.055	0.050		−2.804[m]
0	0				

[a] All potentials in V (± 1–5 mV) *vs.* ferrocenium–ferrocene, *ca.* 20 °C. [b] Formal redox potential of $[C_{10}H_{10-x}Cl_xFe]^{+/0}$ couple. [c] $E_{pa} - E_{pc}$ for $[C_{10}H_{10-x}Cl_xFe]^{+/0}$ couple. [d] Value for ferrocenium–ferrocene under identical conditions. [e] Anodic peak potential (second irreversible oxidation). [f] Cathodic peak potential (irreversible two-electron reduction). [g] 1.5 mm Glassy carbon electrode, 0.100 V s^{-1}. [h] 12.5 μm Platinum microelectrode, 80 V s^{-1}. [i] 5 μm Gold microelectrode, 1 V s^{-1}. [j] 5 μm Gold microelectrode, 160 V s^{-1}. [k] 1.5 mm Glassy carbon electrode, 0.020 V s^{-1}. [l] Ref. 6*a*. [m] In thf–0.1 mol dm^{-3} NBu_4BF_4.

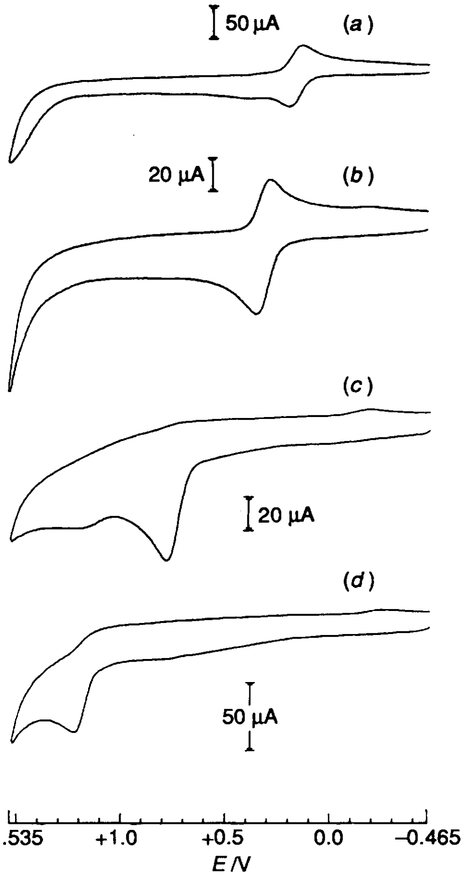

Fig. 1 Cyclic voltammograms of oxidations of 1–2 mmol dm^{-3} $C_{10}H_{10-x}Cl_xFe$ where x = 1 (*a*), 2 (*b*), 5 (*c*) and 10 (*d*), in MeCN–0.1 mol dm^{-3} NBu_4BF_4 at room temperature with a 1.5 mm glassy carbon electrode at 0.100 V s^{-1} (*vs.* ferrocenium–ferrocene). Full *iR* compensation

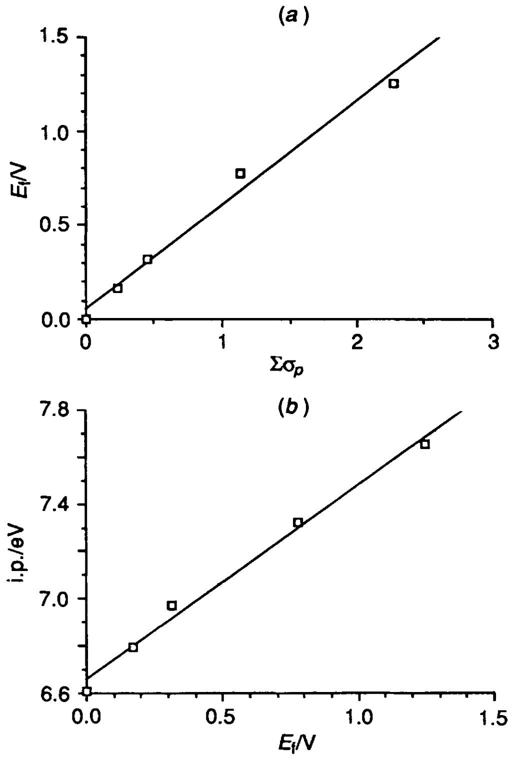

Fig. 2 (*a*) Plot of E_f (*vs.* ferrocenium–ferrocene) for the $[C_{10}H_{10-x}Cl_xFe]^{+/0}$ couples (x = 0, 1, 2, 5 or 10) against the sum of the Hammett *para* coefficient ($\Sigma\sigma_p$) for the chloro substituent. (*b*) Plot of gas-phase first ionisation potentials from ref. 10*m* against E_f; values for x = 1 and 5 obtained *via* interpolation

substituents leads to a significant positive shift in E_f for the $[C_{10}H_{10-x}Cl_xFe]^{+/0}$ couples, with a maximum shift of + 1.246 V *vs.* ferrocenium–ferrocene observed for $[Fe(\eta\text{-}C_5Cl_5)_2]^{+/0}$. Redox potentials for the couples are found to be linearly correlated to $\Sigma\sigma_p$ for the chloro substituent[5a] [Fig. 2(*a*)] with linear regression of the data leading to the empirical relationship (1) between E_f (*vs.* ferrocenium–ferrocene) and $\Sigma\sigma_p$. The

$$E_f/\text{V} = 0.548\ (\Sigma\sigma_p) + 0.052 \qquad (R^2 = 0.992) \qquad (1)$$

correlation coefficient (R^2) is close to unity and indicates that the E_f values obtained are highly correlated to $\Sigma\sigma_p$ (*i.e.* the number of chloro substituents). This suggests that the electronic influence of the chloro substituent on E_f is additive and largely independent of the other substituents. The shift in E_f per chloro substituent actually decreases slightly in a monotonic fashion with increased chlorination, as do the first gas-phase ionisation potentials for the complexes $[Fe(C_5H_{5-n}Cl_n)_2]$ (n = 1–5) in a study by Barfuss *et al.* (see Fig. 4 of ref. 10*m*). Such obervations are consistent with the chloro substituents interacting with one another to a small extent as may be expected by their high negative ionicities.[10e] When the ionisation potentials (i.p.s.) obtained from ref. 10*m* are plotted against E_f for the chlorinated ferrocenes [Fig. 2(*b*)] the two values are also found to be highly correlated (i.p./eV = 0.821E_f + 6.557; R^2 = 0.990). Ionisation potentials for chlorinated ferrocenes have also been found to correlate linearly with both $\Sigma\sigma_p$ and E_f in previous studies.[6b,10i,m] The usefulness of this latter type of correlation applied to metallocenes in general has also been expressed.[3,11]

The high correlation between the free energies of condensed-

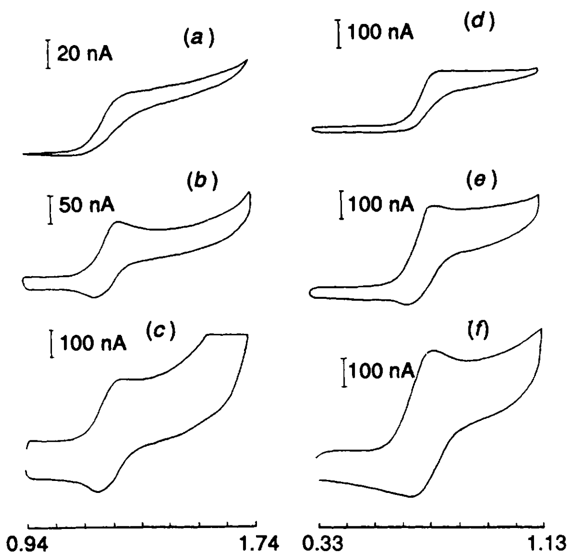

Fig. 3 Cyclic voltammograms in MeCN–0.1 mol dm^{-3} NBu_4BF_4 (*ca.* 20 °C) for the oxidation of *ca.* 1 mmol dm^{-3} $[Fe(\eta\text{-}C_5Cl_5)_2]$ at 0.16 (*a*), 16 (*b*) and 80 V s^{-1} (*c*) all at 12.5 μm Pt, and of 5 mmol dm^{-3} $[Fe(\eta\text{-}C_5H_5)(\eta\text{-}C_5Cl_5)]$ at 16 (*d*), 80 (*e*) and 160 V s^{-1} (*f*) all at 5 μm gold (*vs.* ferrocenium–ferrocene). No *iR* compensation

phase redox potentials ($\Delta G^{\circ\prime} = -nFE_f$) and the gas-phase ionisation potentials suggests that it is predominantly the stabilisation of the occupied molecular orbitals of the chlorinated ferrocenes (and not solvation effects) that leads to the observed linear increases in E_f with ionisation potential. Such stabilisation of the $C_{10}H_{10-x}Cl_xFe$ e_{2g} redox orbital (mainly d-orbital character in ferrocene)[3,10h] has been attributed to increased hybridisation between the Fe $d_{x^2-y^2}$, d_{xy} orbitals and the cyclopentadienyl (e_{2g})-Π orbitals in $C_{10}H_{10-x}Cl_xFe$ relative to ferrocene.[10i] The strong electron-withdrawing properties of the chloro substituents presumably allow greater overlap and mixing of the iron and cyclopentadienyl orbitals yielding a more stable electron configuration. This is borne out by several investigations by Phillips and co-workers which include (*i*) the increased metal–ring stretching force constants, derived for the chlorinated ring of these molecules, compared to the ferrocene value,[10k] (*ii*) the assignment of electric dipole vectors for the metal–ring bonds,[12a] and (*iii*) the polarisation relaxation times for internal ring rotation in $[Fe(\eta\text{-}C_5H_5)(\eta\text{-}C_5H_4Cl)]$, $[Fe(\eta\text{-}C_5H_4Cl)_2]$ and $[Fe(\eta\text{-}C_5H_5)(\eta\text{-}C_5Cl_5)]$.[12b]

Microelectrode and High-scan-rate Electrochemistry.—Fig. 3 shows cyclic voltammograms obtained at scan rates between 0.160 and 160 V s^{-1} for $[Fe(\eta\text{-}C_5Cl_5)_2]$ and $[Fe(\eta\text{-}C_5H_5)(\eta\text{-}C_5Cl_5)]$ in MeCN–0.1 mol dm^{-3} NBu_4BF_4 using 5 μm gold and 12.5 μm platinum microelectrodes. The voltammograms of Fig. 3(*a*) and 3(*d*) indicate irreversible oxidation of both couples at the low scan rates. As the scan rate was increased (between 16 and 160 V s^{-1}) peak-shaped behaviour began to develop for both couples concomitant with an increase in i_{pc}/i_{pa} at the higher scan rates, characteristic of an electrochemical–chemical or similar process (the chemical step being an irreversible homogeneous reaction of the $[C_{10}H_{10-x}Cl_xFe]^+$ cation).[13] The oxidation of $[Fe(\eta\text{-}C_5Cl_5)_2]$ begins to approach chemical reversibility at 80 V s^{-1} [Fig. 3(*c*)] with $E_f = 1.246$ V ($\Delta E_p = 98$ mV, $i_{pc}/i_{pa} = 0.72$, 12.5 μm Pt). For $[Fe(\eta\text{-}C_5H_5)(\eta\text{-}C_5Cl_5)]$ the couple is somewhat less reversible even at 160 V s^{-1} [Fig. 3(*f*)] with $E_f = 0.774$ V ($\Delta E_p = 100$ mV, $i_{pc}/i_{pa} = 0.65$, 5 μm Au), all *vs.* ferrocenium–ferrocene. Cyclic voltammograms of the ferrocenium–ferrocene couple in MeCN–0.5 mol dm^{-3} NBu_4BF_4 at 160 V s^{-1} have $i_{pc}/i_{pa} = 1$, with $\Delta E_p = 83$ (12.5 μm Pt) and 100 mV (5 μm Au).[14] The similarity in ΔE_p values for both $[Fe(\eta\text{-}C_5Cl_5)_2]^{+/0}$ and $[Fe(\eta\text{-}C_5H_5)(\eta\text{-}C_5Cl_5)]^{+/0}$ couples compared to ΔE_p of ferrocenium–ferrocene under similar conditions (within ±15 mV) suggest the chloro couples are electrochemically reversible at these scan rates and, as for $[Fe(\eta\text{-}C_5H_5)_2]^{+/0}$, are one-electron processes.

The variable-scan-rate cyclic voltammograms of $[Fe(\eta\text{-}C_5Cl_5)_2]$ at a 12.5 μm platinum microelectrode [Fig. 3(*a*)–3(*c*)] show the transition from the low-scan-rate diffusion-limited steady-state process [Fig. 3(*a*), 0.160 V s^{-1}] to the peak-shaped response seen at higher scan rates [Fig. 3(*c*) 160 V s^{-1}]. This transition reflects a change from radial to linear diffusion of the electroactive species to the electrode surface at the smaller experimental time-scales.[15] Digital simulation of the data at high scan rates showed that linear diffusion dominated.

The irreversible oxidation of organometallic species are often multielectron processes, with the electrochemical–chemical–electrochemical mechanism being common.[3,16] For reversible one-electron couples, a plot of i_p *vs.* $v^{\frac{1}{2}}$ yields a single slope (proportional to $n^{\frac{3}{2}}$) passing through the origin at (0,0).[13a] Such a plot of i_{pa} for the oxidation of $[Fe(\eta\text{-}C_5H_5)(\eta\text{-}C_5Cl_5)]$ reveals two distinct slopes (gradients m_1 and m_2). At scan rates below 1.6 V s^{-1}, $m_1 = 19.9$ μA s$^{\frac{1}{2}}$ V$^{-\frac{1}{2}}$ ($y_{int} = 1.9$, μA, $R^2 = 0.961$), and at higher scan rates, $m_2 = 10.3$ μA s$^{\frac{1}{2}}$ V$^{-\frac{1}{2}}$ ($y_{int} = 9.7$, μA, $R^2 = 0.960$). For reversible couples the gradient for an $n = 2$ process is 2.8 times that for a one-electron transfer ($2^{\frac{3}{2}}/1^{\frac{3}{2}}$). Considering i_{pa} is larger for a reversible relative to an irreversible process, the m_1/m_2 ratio (1.9:1) suggests a net two-electron process under irreversible conditions (< 10 V s^{-1}) becoming a reversible one-electron transfer above 1.6 V s^{-1}. This is consistent with the observed onset of reversibility of the couple above this scan rate. The ratio $i_{pa}/v^{\frac{1}{2}}$ is similarly proportional to $n^{\frac{3}{2}}$ and a transition in the value of $i_{pa}/v^{\frac{1}{2}}$ from 28.9 to 11.5 μA s$^{\frac{1}{2}}$ V$^{-\frac{1}{2}}$ is observed from low to high scan rates (see SUP 56925), a decrease by a factor of 2.51, characteristic of an electrochemical–chemical–electrochemical mechanism.[13b] For normal electrochemical–chemical reactions $i_p/v^{\frac{1}{2}}$ varies only slightly with v.[16a]

The variable-scan-rate electrochemistry for $[Fe(\eta\text{-}C_5Cl_5)_2]$ was less reproducible than that of $[Fe(\eta\text{-}C_5H_5)(\eta\text{-}C_5Cl_5)]$ owing to the low solubility of the former complex in the solvent and possible concomitant fouling of the very-small-surface-area microelectrodes. In an attempt to increase the solubility of $[Fe(\eta\text{-}C_5Cl_5)_2]$, identical experiments were performed in dmf–0.1 mol dm^{-3} NBu_4BF_4. However, larger charging currents led to a loss of the oxidation signal above 80 V s^{-1} at both 12.5 μm platinum and 0.5 mm gold electrodes. It was also noted that at this scan rate the oxidation was still irreversible.

In MeCN a small irreversible second anodic peak was observed for both $[Fe(\eta\text{-}C_5Cl_5)_2]$ and $[Fe(\eta\text{-}C_5H_5)(\eta\text{-}C_5Cl_5)]$ positive of the initial irreversible oxidation at electrodes of glassy carbon and Au, but not Pt. For the oxidation of $[Fe(\eta\text{-}C_5Cl_5)_2]$ at 1 V s^{-1} with a 5 μm gold microelectrode under steady-state conditions, this appeared as a distinct shoulder at *ca.* 1.53 V (*vs.* ferrocenium–ferrocene), or *ca.* 0.3 V positive of E_{pa} for the $[Fe(\eta\text{-}C_5Cl_5)_2]$ oxidation [Fig. 4(*a*)]. No second oxidation peak was detected at higher scan rates (to 160 V s^{-1}). This second response is more evident for the oxidation of $[Fe(\eta\text{-}C_5H_5)(\eta\text{-}C_5Cl_5)]$ at 0.020 V s^{-1} at a 1.5 mm glassy carbon electrode with a peak potential of 1.148 V, or 0.444 V positive of E_{pa} for the $[Fe(\eta\text{-}C_5H_5)(\eta\text{-}C_5Cl_5)]$ oxidation [Fig. 4(*b*)]. The peak current of this second irreversible oxidation was *ca.* 15% of i_{pa} for the initial $[Fe(\eta\text{-}C_5H_5)(\eta\text{-}C_5Cl_5)]$ oxidation. This second oxidation is most likely due to a decomposition product of the unstable 17-electron $[C_{10}H_{10-x}Cl_xFe]^+$ cation and, due to its absences at platinum electrodes, may be associated with electrode fouling {*cf.* $[Cr(C_6H_6)(CO)_3]^+$}.[16b]

Decomposition Kinetics.—The first-order (pseudo-first-order) rate constants for the decompositions of the $[Fe(\eta\text{-}C_5Cl_5)_2]^+$ and $[Fe(\eta\text{-}C_5H_5)(\eta\text{-}C_5Cl_5)]^+$ cations (k_f) in MeCN–0.1 mol dm^{-3} NBu_4BF_4 at room temperature (*ca.* 20 °C) were determined from the microelectrode data (see above). Using the method of Nicholson and Shain applied to an electrochemical–

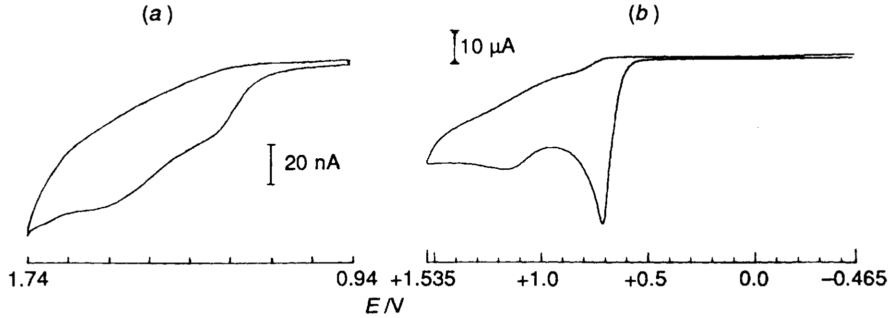

Fig. 4 Cyclic voltammograms of (*a*) *ca.* 1 mmol dm^{-3} [Fe(η-C_5Cl_5)$_2$] at 1 V s^{-1} (5 μm gold microelectrode, no *iR* compensation) and (*b*) 2 mmol dm^{-3} [Fe(η-C_5H_5)(η-C_5Cl_5)] at 0.02 V s^{-1} (1.5 mm glassy carbon electrode, full *iR* compensation) in MeCN–0.1 mol dm^{-3} NBu_4BF_4 at room temperature

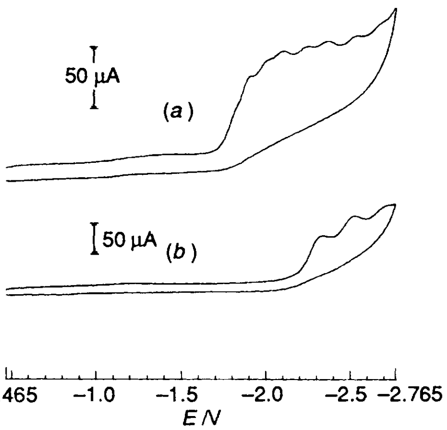

Fig. 5 Cyclic voltammograms of the reduction of 1–2 mmol dm^{-3} [Fe(η-C_5Cl_5)$_2$] (*a*) and [Fe(η-C_5H_5)(η-C_5Cl_5)] (*b*) in MeCN–0.1 mol dm^{-3} NBu_4BF_4 with a 1.5 mm glassy carbon electrode at 0.100 V s^{-1} and at room temperature. Full *iR* compensation

chemical–electrochemical reaction,[13a] k_f was determined to be 40 ± 20 ($t_{\frac{1}{2}}$ = 23 ± 11), and 200 ± 50 s^{-1} (3.7 ± 0.9 ms) for the [Fe(η-C_5Cl_5)$_2$]$^+$ and [Fe(η-C_5H_5)(η-C_5Cl_5)]$^+$ cations, respectively. Digital simulation[17] of experimental cyclic voltammograms as a function of v using the above values of k_f gave good agreement between experimental and observed data. Calculated rate constants at different scan rates and simulated cyclic voltammograms are given in SUP 56925. The results for the [Fe(η-C_5Cl_5)$_2$]$^{+/0}$ couple in dmf show that k_f > 250 s^{-1}.

Nearly all 17-electron organometallic species react *via* attack of nucleophiles upon the electron-deficient species.[18] Due to the presence of strong electron-withdrawing chloro substituents and the very positive E_f values, the 17-electron [$C_{10}H_{10-x}Cl_xFe$]$^+$ cations are expected to act as strong electrophiles,[19] and react with solvent or electrolyte molecules, as is the case for decomposition of the 17-electron cationic species [Cr(C_6H_6)(CO)$_3$]$^+$.[16b] Trace water is unlikely to be the nucleophile as the decomposition rates {for [Fe(η-C_5H_5)(η-C_5Cl_5)] at least} were highly reproducible with different batches of MeCN. Decomposition of the [$C_{10}H_{10-x}Cl_xFe$]$^+$ cations *via* oxidation of the solvent or electrolyte is also unlikely since the much stronger oxidant [Fe(η-C_5Cl_5)$_2$]$^+$ is less reactive. Relative to the results obtained in MeCN, the minimum six-fold increase in k_f of the [Fe(η-C_5Cl_5)$_2$]$^+$ cation obtained in dmf also suggests a solvent-dependent pathway, since dmf is known to be the stronger nucleophile.[20]

Reduction Chemistry.—No reductions of [Fe(η-C_5H_4Cl)$_2$] and [Fe(η-C_5H_5)(η-C_5H_4Cl)] were observed at room temperature in MeCN–0.1 mol dm^{-3} NBu_4BF_4 (1.5 mm glassy carbon electrode) at 0.100 V s^{-1} up to the solvent limit. In tetrahydrofuran–0.1 mol dm^{-3} NBu_4BF_4, however, a single irreversible reduction of [Fe(η-C_5H_5)(η-C_5H_4Cl)] is observed near the solvent limit with an E_{pc} of −2.804 V (*vs.* ferrocenium–ferrocene) under similar conditions. The compounds [Fe(η-C_5Cl_5)$_2$] and [Fe(η-C_5H_5)(η-C_5Cl_5)] both exhibit multiple irreversible reductions in MeCN–0.1 mol dm^{-3} NBu_4BF_4 at 0.100 V s^{-1} (Fig. 5). A total of eight reductions separated by *ca.* 0.1 V are observed for the former at potentials between −1.8 and −2.7 V [Fig. 5(*a*)], whilst three separated by *ca.* 0.2 V are observed for the latter between −2.3 and −2.8 V [Fig. 5(*b*)]; E_{pc} values for all reductions are given in Table 1. No signs of reversible behaviour at higher scan rates (up to 20 V s^{-1}) were observed for either compound, and it is clear that the chloro substituents are reduced before the formation of the anionic species.

Saji and Ito[9b] have reported irreversible two-electron reduction of [Fe(η-C_5H_5)(η-C_5H_4Cl)] at −45 °C in 1,2-dimethoxyethane associated with loss of the chloro substituent. The mechanism of electrochemical reduction of [Fe(η-C_5H_5)(η-C_5H_4X)] (X = Cl, Br or I) as postulated by them involves ring-centred reduction followed by dehalogenation and protonation to yield ferrocene, and a similar mechanism is likely to apply here.

Protonation Chemistry.—The protonation chemistry of ferrocene and derivatives prompted us to investigate whether either [Fe(η-C_5Cl_5)$_2$] or [Fe(η-C_5H_5)(η-C_5Cl_5)] was susceptible to similar protonation.[2,4b,21] Treatment of both complexes with neat anhydrous trifluoromethanesulfonic (triflic) acid resulted in quite different reactivities. The former was slightly soluble in triflic acid giving a stable pale yellow solution consistent with the maintenance of the integrity of the molecule. Only slight decolouration of the solution was observed after 2 d. Treatment of the latter with triflic acid resulted in an immediate colour change from yellow to deep brown, and then to black within minutes. The ^1H NMR singlet at δ 2.63 in the $CDCl_3$[22] solution (five equivalent protons on the unsubstituted cyclopentadienyl ring) was replaced in the acid solution by three broad resonances at δ 5.12, 2.19 and 0.79 (all *vs.* $SiMe_4$) most likely as a result of decomposition of the complex. No high-field hydride resonances were detected for either complex in the acid. The lack of a hydride resonance suggests that protonation to form the hydride complex of [Fe(η-C_5Cl_5)$_2$] is unlikely.[23] Decomposition of [Fe(η-C_5H_5)(η-C_5Cl_5)] under the conditions precludes comment on potential protonation, although protonation to form the hydride complex is likely to be the first step of decomposition.[24]

Conclusion

The decachloro- and 1,2,3,4,5-pentachloro-ferrocenes exhibit interesting electrochemistries in acetonitrile, mainly as a consequence of the strong electron-withdrawing properties of the chloro substituents. The very high correlation between E_f and ionisation potentials for the molecules (including the 1,1′-dichloro- and monochloro-ferrocenes) implicates stabilisation of the e_{2g} redox orbital through increased hybridisation and ligand contribution relative to ferrocene. The striking difference in the rates and thermodynamics of electrophilic attack at $[Fe(\eta\text{-}C_5Cl_5)_2]$ and $[Fe(\eta\text{-}C_5H_5)(\eta\text{-}C_5Cl_5)]$ (protonation) is in contrast with the small differences in the rate constants of decomposition of the corresponding cations. This is consistent with the protonation being metal-ion centred, while the nucleophilic attack at the cations is likely to be centred at the $C_5Cl_5^-$ rings. The chlorinated ferrocenes have also been found to exhibit irreversible two-electron reductions involving the loss of chloro substituents at room temperature. This could be used to study the electrochemistries of chloro complexes of intermediate degrees of substitution.

Experimental

Synthesis.—The mono-, di-, penta- and deca-chloroferrocenes were prepared as reported previously.[10k] Ferrocene (Fluka, Buchs, purum) was used as received. The salt NBu_4BF_4 was prepared by the literature method, recrystallised three times from ethyl acetate–diethyl ether[25] and stored *in vacuo* in the dark.

Solvents and Reagents.—Acetonitrile (Merck, AR grade) was dried and distilled from CaH_2 under N_2; HPLC-grade (Aldrich) MeCN and dmf were used as received. Tetrahydrofuran (thf) (Merck, AR grade) was dried and distilled from sodium wire and benzophenone. All electrochemical solvents were stored under argon (high purity, CIG) in the dark and were purged with argon for at least 30 min prior to use. Trifluoromethanesulfonic acid (Fluka, AR grade) were used as received. Molecular sieves (0.4 nm, Aldrich) was dehydrated by heating to 150 °C in a vacuum oven and was stored under argon. Activated alumina (Catapal^R, Vista) was used as received.

Electrochemistry.—For conventional electrochemical experiments (< 1 V s^{-1}) a BAS-100 Electrochemical Analyzer employing a three-electrode system with 80–100% *iR* compensation was used. The working electrodes were 1.5 mm (radius) glassy carbon and 1 mm platinum embedded disk electrodes. They were regularly polished using a suspension of alumina (0.04 μm, Struers, FF-Alumina) and distilled water on a suede cloth (Struers, DP-Nap) followed by *ca.* 30 s sonication in the organic solvent and a final polish on dry suede cloth. Above 1 V s^{-1} a three-electrode system consisting of a Schlumberger 1186 (Solartron) potentiostat, an Exact 628 (Dynatech, Nevada) analogue function generator, and a Gould 4072 digital storage oscilloscope was used. Data were transferred to an 80286 IBM compatible computer from the oscilloscope with an IEEE interface using ASYST software[26] and a locally written storage and manipulation program.[27] For microelectrode experiments a locally built medium-speed pre-amplifier based on an OPA 606 integrated circuit was used as an input stage to the potentiostat,[28] and no *iR* compensation was used. The pre-amplification gain was varied using a variable feed-back resistor (R_f) which was varied between 10^6 and 10^8 Ω. All microelectrode experiments were performed in an aluminium Faraday cage. Embedded-disk microelectrodes (5 μm radius Au and 12.5 μm radius Pt) were constructed from high-purity wire (Goodfellow Metals, Cambridge, UK; 99.9%).[28,29] A commercially available gold-disk electrode (0.5 mm, Cypress) was also used. Microelectrodes were polished on wet emery-paper (P150 through to P1200), then diamond paste (6 through to 0.1 μm, Hyprez) on a suede cloth to ensure a mirror finish on the surface. Subsequently they were thoroughly polished between scans as for macroelectrodes.

All electrochemical experiments employed a platinum-wire counter electrode and a Ag–AgCl–KCl (saturated) reference electrode, and potentials were internally referenced *versus* the IUPAC standard, ferrocenium–ferrocene.[7] Electrochemistry was performed at concentrations of 1–5 mmol dm^{-3} of electroactive species with either activated alumina or molecular sieves added to the cell to minimise contamination by water. Owing to the low solubility of $[Fe(\eta\text{-}C_5Cl_5)_2]$ in MeCN–0.1 mol dm^{-3} NBu_4BF_4 a saturated solution of the complex was obtained by sonication in a sealed flask under argon for 30 min prior to the electrochemistry. All samples were purged and kept under a continuous flow of argon prebubbled through 0.2 mol dm^{-3} Cr^{2+}, 0.5 mol dm^{-3} $HClO_4$ over Zn/Hg and a sulfuric acid bubbler (18 mol dm^{-3}, reagent grade) to remove all traces of O_2 and water, respectively. The argon was finally saturated with the organic solvent by bubbling through the solvent stored over molecular sieves.

All voltammograms were obtained at room temperature (in duplicate where possible). Experimental i_{pc}/i_{pa} ratios used in the calculations of k_f were obtained from the voltammograms by manual subtraction of the charging current and solvent response. The method of Nicholson and Shain[13a] was then used to calculate k_f at various i_{pc}/i_{pa} values, where the error in k_f is ± 5% applied to an electrochemical–chemical–electrochemical reaction.[13c] Owing to the reproducibility problems associated with the $[Fe(\eta\text{-}C_5Cl_5)_2]^{+/0}$ couple, the decomposition rate for the cation was calculated at only two scans whilst an average over 13 scan rates was used for the $[Fe(\eta\text{-}C_5H_5)(\eta\text{-}C_5Cl_5)]^+$ cation. Cyclic voltammograms were digitally simulated using the program CYCLIC assuming linear diffusion to a disk electrode.[17] Simulations were for an electrochemical (E_1)–chemical–electrochemical (E_2) reaction where E_1 (E_f for the $[C_{10}H_{10-x}Cl_xFe]^{+/0}$ couple) is more positive than E_2 (both $n = 1$) with voltammograms insensitive to the magnitude of E_2. The digital simulations consisted of 200 data points employing the full integral kinetic algorithm. The heterogeneous electron-transfer rate (k_{het}) was assumed to be fast (1 cm s^{-1}), the transfer coefficient (α) was set at 0.5, and a value of 2.4×10^{-5} cm^3 s^{-1} was used for the diffusion coefficients (D) of all species.[5b] All i_{pc}/i_{pa} ratios were calculated from the empirical relationship as derived by Nicholson.[30]

NMR Spectroscopy.—Proton NMR spectra of $[Fe(\eta\text{-}C_5Cl_5)_2]$ and $[Fe(\eta\text{-}C_5H_5)(\eta\text{-}C_5Cl_5)]$ in neat trifluoromethanesulfonic acid were obtained using a Bruker EM-360 spectrometer operating at 60 MHz at room temperature. Resonances are in ppm upfield of $SiMe_4$ obtained *via* internal reference in D_2O in a sealed capillary.

Acknowledgements

P. A. L. gratefully acknowledges funding from the Australian Research Council and a University of Sydney Special Research Grant. Supply of the cyclic voltammogram simulation program CYCLIC by Dr. Robert Binstead is gratefully acknowledged.

References

1 T. J. Keally and P. L. Pauson, *Nature (London)*, 1951, **168**, 1039; S. A. Miller, J. A. Tebboth and J. F. Tremaine, *J. Chem. Soc.*, 1952, 632.
2 M. Rosenblum, *Chemistry of the Iron Group Metallocenes*, Interscience, New York, 1965, part 1.
3 V. V. Strelets, *Coord. Chem. Rev.*, 1992, **114**, 1 and refs. therein.
4 (*a*) M. D. Morris and G. L. Kok, *Encyclopedia of Electrochemistry of the Elements*, Marcel Dekker, New York, 1979, ch. XIII-I; (*b*) A. J. Deeming, *Comprehensive Organometallic Chemistry*, eds. G. Wilkinson, F. G. A. Stone and E. W. Abel, 1st edn., Pergamon, Oxford, 1982, vol. 4, pp. 475–484; (*c*) S. P. Gubin, *Pure Appl. Chem.*, 1970, **23**, 463; (*d*) D. W. Slocum and C. R. Ernst, *Adv. Organomet. Chem.*, 1972, **10**, 79.
5 (*a*) D. H. McDaniel and H. C. Brown, *J. Org. Chem.*, 1958, **23**, 420; (*b*) T. Kuwana, D. E. Bublitz and G. Hoh, *J. Am. Chem. Soc.*, 1960, **82**, 5811; (*c*) D. W. Hall and C. D. Russel, *J. Am. Chem. Soc.*, 1967, **89**, 2316.
6 (*a*) W. E. Britton, R. Kashyap, M. El-Hashash, M. El-Kady and M. Herberhold, *Organometallics*, 1986, **5**, 1029; (*b*) A. M. Al-Saeed, E. A. Seddon, K. R. Seddon, A. A. Shimran and S. Tompkins, *J. Organomet. Chem.*, 1988, **347**, C25.
7 IUPAC, Commission on Electrochemistry, in *Pure Appl. Chem.*, 1984, **56**, 461.

8 Y. Mugnier, C. Moise, J. Tirouflet and E. Laviron, *J. Organomet. Chem.*, 1980, **186**, C49; N. Ito, T. Saji and S. Aoyagui, *J. Organomet. Chem.*, 1983, **247**, 301.

9 (*a*) N. El Murr and A. Chaloyard, *J. Organomet. Chem.*, 1980, **193**, C60; (*b*) T. Saji and N. Ito, *Bull. Chem. Soc. Jpn.*, 1985, **58**, 3375.

10 (*a*) L. D. Smithson, A. K. Bhattacharya and F. L. Hedberg, *Org. Mass Spectrom.*, 1970, **4**, 383; (*b*) Y. S. Sohn, D. N. Hendrickson and H. B. Gray, *J. Am. Chem. Soc.*, 1971, **93**, 3603; (*c*) S. Evans, M. L. H. Green, B. Jewitt, A. F. Orchard and C. F. Pygall, *J. Chem. Soc., Faraday Trans. 2*, 1972, 1847; (*d*) F. L. Hedberg and H. Rosenberg, *J. Therm. Anal.*, 1974, **6**, 571; (*e*) I. Motoyama, N. Shimojima, S. Iijima and H. Sano, *Chem. Lett.*, 1976, **11**, 1257; (*f*) S. Ikuta, I. Motoyama and H. Sano, *Radiochem. Radioanal. Lett.*, 1983, **58**, 329; (*g*) T. Vondrák, *J. Organomet. Chem.*, 1984, **275**, 93; (*h*) R. M. G. Roberts and J. Silver, *J. Organomet. Chem.*, 1984, **263**, 235; (*i*) D. C. Driscoll, P. A. Dowben, N. M. Boag, M. Grade and S. Barfuss, *J. Chem. Phys.*, 1986, **85**, 4802; (*j*) S. Barfuss, M. Grade, W. Hirschwald, W. Rosinger, N. M. Boag, D. C. Driscoll and P. A. Dowben, *J. Vac. Sci. Technol. A*, 1987, **5**, 1451; (*k*) L. Phillips, A. R. Lacey and M. K. Cooper, *J. Chem. Soc., Dalton Trans.*, 1988, 1383; (*l*) P. A. Dowben, D. C. Driscoll, R. S. Tate and N. M. Boag, *Organometallics*, 1988, **7**, 305; (*m*) S. Barfuss, K. H. Emrich, W. Hirschwald, P. A. Dowben and N. M. Boag, *J. Organomet. Chem.*, 1990, **391**, 209.

11 V. V. Strelets and S. V. Kukharenko, *Nouv. J. Chim.*, 1984, **8**, 785.

12 L. Phillips and S. W. Filipczuk, *J. Mol. Liq.*, (*a*) 1991, **47**, 261; (*b*) in the press.

13 R. S. Nicholson and I. Shain, *Anal. Chem.*, (*a*) 1964, **36**, 706; (*b*) 1965, **37**, 178; (*c*) 1965, **37**, 190.

14 P. T. Gulyas, B.Sc. (Hons) Thesis, University of Sydney, 1990.

15 R. M. Whightman and D. O. Wipf, *Acc. Chem. Res.*, 1990, **23**, 64.

16 (*a*) Southampton Electrochemistry Group, *Instrumental Methods in Electrochemistry*, Ellis Horwood, Chichester, 1985, ch. 6, pp. 189–200; (*b*) C. G. Zoski, D. A. Sweigart, N. J. Stone, P. H. Rieger, E. Mocellin, T. F. Mann, D. R. Mann, D. K. Gosser, M. M. Doeff and A. M. Bond, *J. Am. Chem. Soc.*, 1988, **110**, 2109.

17 R. A. Binstead, M. R. Bruce and B. P. Sullivan, CYCLIC, Version 4.0, University of North Carolina, NC, 1990.

18 D. A. Sweigart, *Mechanisms of Inorganic and Organometallic Reactions*, ed. M. V. Twigg, Plenum, New York, 1985, ch. 10, pp. 263–281; L. A. P. Kane-Maguire, E. D. Honig and D. A. Sweigart, *Chem. Rev.*, 1984, **84**, 525 and refs. therein.

19 A. J. Birch, D. Bogsanyi and L. F. Kelly, *J. Organomet. Chem.*, 1981, **214**, C39.

20 C. Degrand and A. Radecki-Sudre, *J. Organomet. Chem.*, 1984, **268**, 63; C. Degrand, A. Radecki-Sudre and J. Besancon, *Organometallics*, 1982, **1**, 1311.

21 W. E. Watts, *Comprehensive Organometallic Chemistry*, 1st edn., eds. G. Wilkinson, F. G. A. Stone and E. W. Abel, Pergamon, Oxford, 1982, vol. 8, pp. 1025, 1026.

22 F. L. Hedberg and H. Rosenberg, *J. Am. Chem. Soc.*, 1973, **95**, 870.

23 T. J. Curphey, J. O. Santer, M. Rosenblum and J. H. Richards, *J. Am. Chem. Soc.*, 1960, **82**, 5249; J. Kotz and D. Pedrotty, *Organomet. Chem. Rev. A*, 1969, **4**, 479.

24 M. Rosenblum, J. O. Santer and W. G. Howells, *J. Am. Chem. Soc.*, 1963, **85**, 1450.

25 A. E. Rehan, R. A. Barkhau and J. M. Williams, *Inorg. Synth.*, 1986, **24**, 139; R. Moulton, T. W. Weidman, K. P. C. Vollhardt and A. J. Bard, *Inorg. Chem.*, 1986, **25**, 1846.

26 ASYST, Macmillan Software Company, Version 2.0, Adaptable Laboratory Software, Rochester, NY, 1987.

27 P. T. Gulyas and D. Fleming, GPIB, University of Sydney, 1991.

28 N. S. McAlpine, unpublished work.

29 K. Dubinska, B.Sc. (Hons) Thesis, University of Sydney, 1987.

30 R. S. Nicholson, *Anal. Chem.*, 1966, **38**, 1406.

Received 31*st July* 1992; *Paper* 2/04137E